ELSEVIER

Journal of Chromatography A, 849 (1999) 45–60

JOURNAL OF CHROMATOGRAPHY A

Estimation of the adsorption energy distributions for the Jovanovic–Freundlich isotherm model with Jovanovic local behavior

Igor Quiñones[a,c], Brett Stanley[d], Georges Guiochon[b,c,*]

[a]*Department of Chemical Engineering, The University of Tennessee, Knoxville, TN 37996-1600, USA*
[b]*Department of Chemistry, The University of Tennessee, Knoxville, TN 37996-1600, USA*
[c]*Division of Chemical and Analytical Sciences, Oak Ridge National Laboratory, Oak Ridge, TN 37831-6120, USA*
[d]*Department of Chemistry, California State University, San Bernardino, CA 92407-2397, USA*

Received 27 November 1998; received in revised form 9 April 1999; accepted 9 April 1999

Abstract

The successful design of many modern separation processes as the overloaded chromatographic separations require an accurate knowledge of the associated adsorption equilibria. It is well known that the characterization of the adsorbent heterogeneity plays an important role in the understanding of the adsorption equilibria. In a previous paper, a new Jovanovic–Freundlich isotherm model for single-component adsorption on heterogeneous surfaces was proposed. Also, the adsorption energy distributions (AEDs) corresponding to the new model for Langmuir local behavior were derived and evaluated for the specific case of the adsorption of a series of chlorinated hydrocarbons on silica gel. In the present study, the adsorption energy distributions corresponding to the Jovanovic–Freundlich model with Jovanovic local behavior are evaluated for the same set of experimental data. In order to provide a basis for comparison, adsorption energy distributions were also estimated for the given set of data via an established expectation–maximization procedure which does not assume any particular model for the overall isotherm. The results presented in these paper complement the previous findings and provide new insights into the features of the Jovanovic–Freundlich isotherm model, which could be useful both in the correlation of single-component adsorption data and in the prediction of multicomponent equilibria.

Keywords: Adsorption isotherms; Jovanovic–Freundlich isotherms; Adsorption energy distributions; Thermodynamic parameters; Organochlorine compounds

1. Introduction

The application of adsorption-based processes like industrial-scale preparative chromatography is becoming common in industry [1]. The design and optimization of an adsorption-based process require the knowledge of the adsorption equilibria of the species involved in the separation [2]. The experimental determination of competitive equilibrium data is costly and time-consuming. There are methods that allow estimation of the multicomponent equilibria from the analysis of single component data [3]. Most of the adsorbents employed in industrial applications exhibit surface and structural heterogeneities [4]. Thus, the assessment of the adsorbent heterogeneity from the analysis of single

*Corresponding author. Tel.: +1-423-974-0733; fax: +1-423-974-2667.
E-mail address: guiochon@utk.edu (G. Guiochon)

0021-9673/99/$ – see front matter
PII: S0021-9673(99)00509-9

component data is an important part of the existing models for the prediction of multicomponent adsorption equilibria [4–6]. The adsorbent heterogeneity can be formally described by a distribution of homogeneous sites with different energies, known as the adsorption energy distribution (AED). The adsorption on the sites with the same energy is characterized using an isotherm model valid for an homogeneous surface, known as the local isotherm model. In a previous publication [7], a Jovanovic–Freundlich (JF) isotherm model for single component adsorption on heterogeneous surfaces was proposed. The model was applied to the analysis of published adsorption data of several chlorinated hydrocarbons on silica gel [8,9] in order to derive by regression the corresponding isotherm parameters. Also, an analytical expression for the AED corresponding to the JF model for Langmuir local behavior was derived following the procedure proposed by Sips [8].

The aim of this paper is to provide the calculated AED corresponding to the JF model for Jovanovic local behavior, taking into account that the former reduces to the latter for the particular case of an homogeneous surface. Also, AEDs were calculated from the experimental adsorption data using an established expectation maximization (EM) procedure [11,12] which does not require prior knowledge of the overall adsorption isotherm. The EM method requires the assumption of a local isotherm model and in the particular case of this study, the AEDs were calculated for both Jovanovic and Langmuir local behavior. Therefore, a comparison between the AEDs calculated from the JF model and from other reported procedures is carried out. This comparison is important in order to check the consistency of the AEDs generated by the new model.

2. Theory

The overall (or experimental) isotherm is the result of the summation of the adsorption taking place over all the homogeneous sites of different energies. This sum can be replaced by an integral provided that there exists a continuous AED. Then the overall isotherm on the heterogeneous surface can be described by the following integral equation [4]

$$\Theta(P) = \frac{q}{q_s} = \int_0^\infty \theta(P,\epsilon)\ \lambda(\epsilon)\ \mathrm{d}\epsilon \tag{1}$$

where $\Theta(P)$ is the overall fractional coverage, a function of the partial pressure P of the adsorbate, q is the specific amount adsorbed, q_s is the saturation or monolayer capacity of the adsorbent, $\theta(P, \epsilon)$ is the local fractional coverage on sites of energy ϵ and $\lambda(\epsilon)$ is the AED.

The Jovanovic–Freundlich model is described by the expression [7]

$$\Theta(P) = 1 - \mathrm{e}^{-(a\,P)^{\nu}} \tag{2}$$

where ν is the heterogeneity parameter and a is a temperature-dependent parameter described by the equation [7]

$$a = K^0\,\mathrm{e}^{\frac{\epsilon_a}{RT}} \tag{3}$$

where K^0 is a preexponential parameter, ϵ_a is the characteristic energy of the distribution, R the ideal gas constant, and T the absolute temperature. The values of the parameters K^0 and ϵ_a can be determined from a linear plot of Eq. (3) provided that isotherm data is available at different temperatures [7]. The Jovanovic–Freundlich model described by Eq. (2) reduces, for the particular case of an homogeneous surface ($\nu = 1$) to the well known Jovanovic model [13]

$$\theta(P,\epsilon) = 1 - \mathrm{e}^{-(K\,P)} \tag{4}$$

where the Henry law constant K is described by the expression [4]

$$K = K_0\,\mathrm{e}^{\frac{\epsilon}{RT}} \tag{5}$$

In the previous expression, K_0 is a preexponential factor dependent on the molecular partition functions of the adsorbate in both the bulk and adsorbed phases. In this study we used an expression for K_0 proposed by Jaroniec [14]

$$K_0 = \frac{\mathrm{e}^{-\frac{H_{\mathrm{vap}}}{RT}}}{P_s} \tag{6}$$

where P_s is the vapor pressure and H_{vap} is the heat of vaporization of the adsorbate, both values evaluated at temperature T.

To estimate the energy distributions corresponding to the Jovanovic–Freundlich model for the Jovanovic local behavior, let introduce the variable Z, defined as [15]

$$Z = e^{\frac{\epsilon}{RT}} - 1 \tag{7}$$

Combining Eqs. (1), (4), (5) and (7) and considering the normalization condition [4]

$$\int_0^\infty \lambda(\epsilon)\, d\epsilon = 1 \tag{8}$$

we obtain [15]

$$\Theta(P) = 1 - RT\, e^{-K_0 P} \int_0^\infty \lambda(Z)\, e^{-K_0 P Z}\, dZ \tag{9}$$

where $\lambda(Z) = \frac{\lambda(\epsilon)}{1+Z}$ and obviously $\epsilon = RT\ \ln(Z+1)$ (Eq. (7)). Note that the integrand in the right-hand-side of Eq. (9) has the form of the Laplace transform [16]

$$F(s) = \int_0^\infty \lambda(Z)\, e^{-sZ}\, dZ \tag{10}$$

where $F(s)$ is a function of the complex argument $s = K_0 P$. Combining Eqs. (2), (9), and (10), we derive the function $F(s)$ corresponding to the Jovanovic–Freundlich model as

$$F(s) = \frac{1}{RT}\, e^{-(\frac{as}{K_0})^\nu + s} \tag{11}$$

Knowing the function $F(s)$ defined by Eq. (11) permits the inversion of the Laplace transform (Eq. 10), the derivation of the functional relationship $\lambda(Z)$, and from there, that of the AED, i.e. $\lambda(\epsilon)$. The AED can also be obtained by direct inversion of Eq. (1). Both Eqs. (1) and (10) belong to the class of linear Fredholm integral equations of the first kind. Their numerical inversion is usually a mathematically ill-posed problem. The EM method is an iterative maximum-likelihood procedure which has the advantages of permitting the derivation of a statistically robust estimate of the AED and of requiring no smoothing of the isotherm data but of operating directly on the raw isotherm data. In the solution of Eq. (1), the AED is directly evaluated from M experimental adsorption data points at N energy grid points. Eq. (1) is evaluated using the expression [11,12]

$$q_{cal}(P_j) = \sum_{\epsilon_{min}}^{\epsilon_{max}} \lambda(\epsilon_i)\theta(P_j,\epsilon_i)\, \Delta\epsilon \tag{12}$$

for $i = 1,2,\ldots,N$, $j = 1,2,\ldots,M$ and where $\Delta\epsilon$ is the energy grid spacing. In the previous expression, ϵ_{min} and ϵ_{max} correspond to the lower and upper boundaries of the evaluated AED, respectively. The AED is updated at the k iteration using the expression [11,12]

$$\lambda^{k+1}(\epsilon_i) = \lambda^k(\epsilon_i) \sum_{P_{min}}^{P_{max}} \theta(P_j,\epsilon_i)\, \Delta\epsilon\, \frac{q_{exp}(P_j)}{q_{cal}(P_j)} \tag{13}$$

where q_{exp} is the experimental value of solid-phase concentration. The usual initial guess of the AED in Eq. (12) is the uniform distribution [11,12]. This initial estimate introduces the minimum bias into the calculated AED. The EM method applied in this study employed as local models either the Jovanovic model represented by Eq. (4) or the Langmuir model [19], namely

$$\theta(P, \epsilon) = \frac{KP}{1+KP} \tag{14}$$

The EM procedure is a reasonable choice which protects better than most other methods against the consequences of possible experimental artifacts which can be incorporated in the calculation of AED or against the effect of modeling the experimental data or the AED [12].

3. Results

The values of the parameters q_s, a and ν at different temperatures were derived and reported previously (see Table 3 from Ref. [7]), as a result of the regression analysis of the experimental data of chlorinated hydrocarbons obtained by Hines et al. [9,10]. The values of these parameters were used in Eq. (11) in order to invert numerically the Laplace transform and derive the corresponding AEDs. The value of the preexponential factor required in Eq. (11) was calculated from Eq. (6) using reported values of P_s and H_{vap} at the desired temperatures [17]. The numerical inversion was accomplished

using the INLAP subroutine from the IMSL MATH/LIBRARY [18]. Figs. 1a–6a show these calculated AEDs for all the systems which were analyzed previously [7]. The normalization condition (8) was checked for every calculated AED. The results of the integration by (8) are exposed in the third column of Table 3 ($\int \lambda_{JF}(\epsilon)\, d\epsilon$). The value of the energy for which these AEDs distributions are maximum ($\epsilon_{a,JF}$) are reported in the third column of Table 1. For the sake of comparison, the heats of vaporization (H_{vap}) and the experimental isosteric heats of adsorption (H_{iso}) previously reported by Hines et al. [9,10] are shown in Figs. 1–6.

The AEDs calculated using the EM method are reported for Jovanovic local behavior in Figs. 1b–6b and for Langmuir local behavior in Figs. 1c–6c. One hundred energy points were employed to extract the solution. Ten thousand iterations were performed to progress toward the maximum likelihood solution over the energy range chosen [12]. At low energies the AED is bounded (ϵ_{min}) by the value of the heat of vaporization, so this constraint was included in the calculations ($\epsilon_{min} = H_{vap}$). The value of ϵ_{max} was selected in order to produce an energy range which results from a compromise between the range which gave the best fit and the range which yielded a

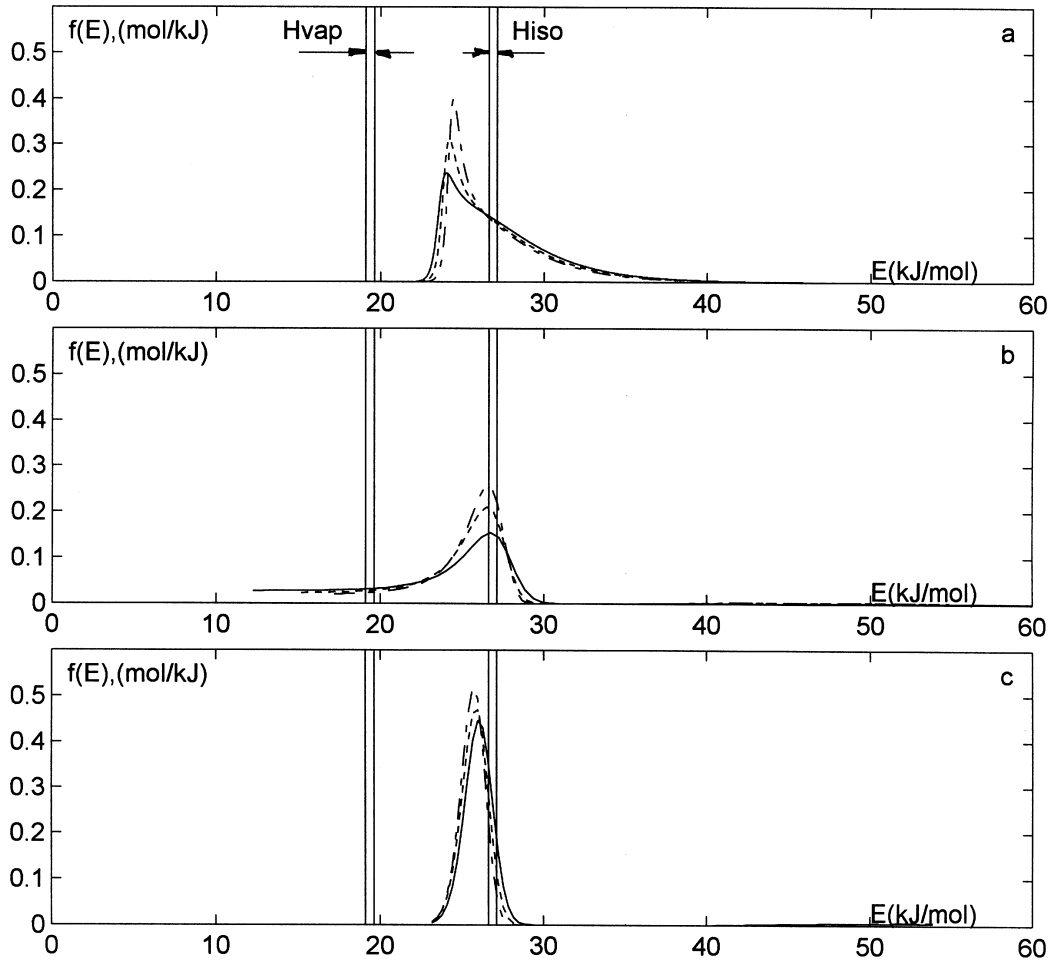

Fig. 1. Adsorption energy distributions of CH_3Cl at 288K (solid line), 293K (short-dashed line) and 298K (long-dashed line) calculated for the Jovanovic–Freundlich model (a), by the EM method with the Jovanovic isotherm as local model (b) and by the EM method with the Langmuir isotherm as local model (c).

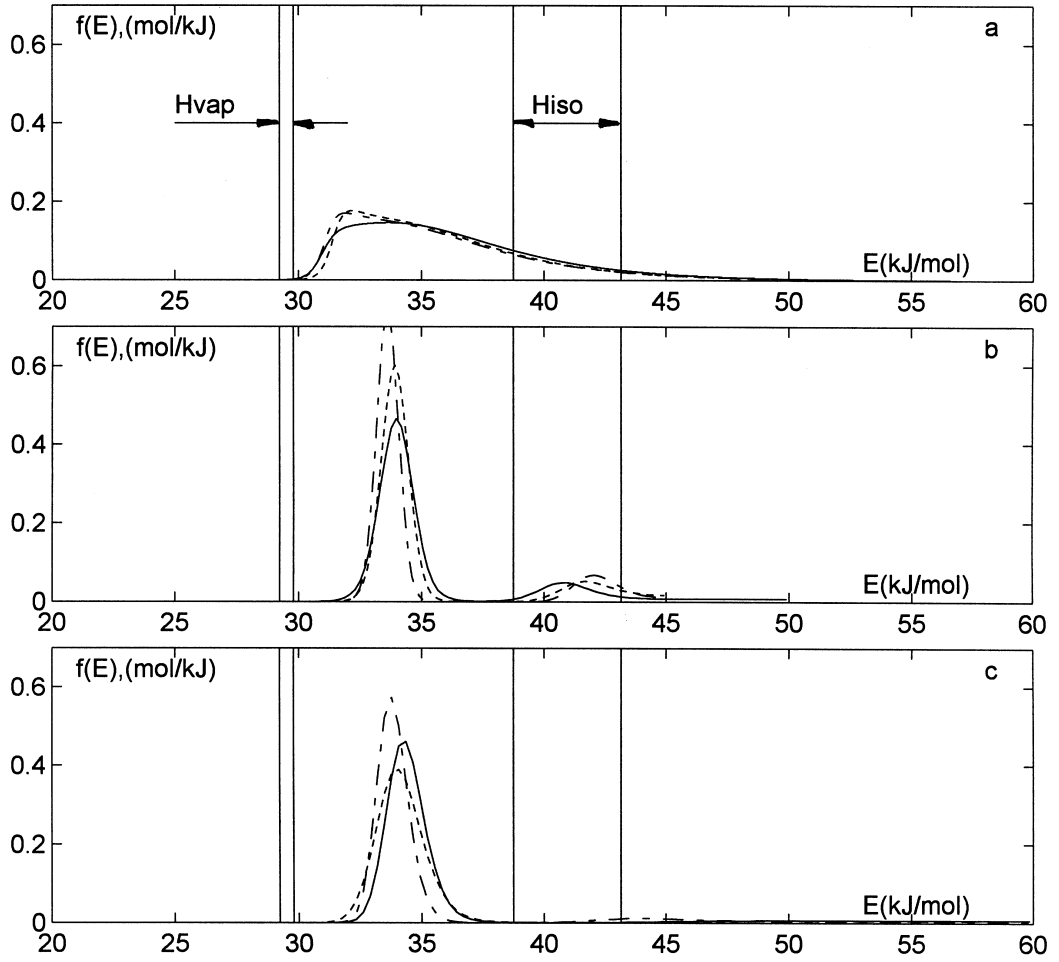

Fig. 2. Adsorption energy distributions of CH_2Cl_2 at 288K (solid line), 293K (short-dashed line) and 298K (long-dashed line) calculated for the Jovanovic–Freundlich model (a), by the EM method with the Jovanovic isotherm as local model (b) and by the EM method with the Langmuir isotherm as local model (c).

well-characterized peak. The upper value for every specific case corresponds to the highest value displayed in Figs. 1–6. The check of the normalization condition (8) is exposed in columns 4 and 5 of Table 3 for the Jovanovic ($\int \lambda_J(\epsilon)\, d\epsilon$) and Langmuir ($\int \lambda_L(\epsilon)\, d\epsilon$) local behavior, respectively. The values of the saturation capacity were obtained by integrating the calculated AEDs. The values of the monolayer capacity extracted from the AEDs in the case of Langmuir local behavior ($q_{s,L}$) are reported in column 3 of Table 2. The values of the saturation capacities corresponding to Jovanovic local behavior ($q_{s,J}$) are reported in column 6 of Table 2. The mean energy values of the main energy peak, calculated as the first moment of this peak are given in columns 4 and 7 of Table 2 for Langmuir ($\epsilon_{mean,L}$) and Jovanovic ($\epsilon_{mean,J}$) local behavior, respectively. The root-square-mean-deviation (δ) was calculated as

$$\delta = \sqrt{\sum \left(\frac{q_{exp} - q_{cal}}{q_{exp}} \right)^2} \qquad (15)$$

It is reported for the overall Jovanovic–Freundlich model (δ_{JF}) in column 4 of Table 1. The AEDs derived from the JF model were then used in Eq. (1) together with Eqs. (4)–(6) in order to recover the

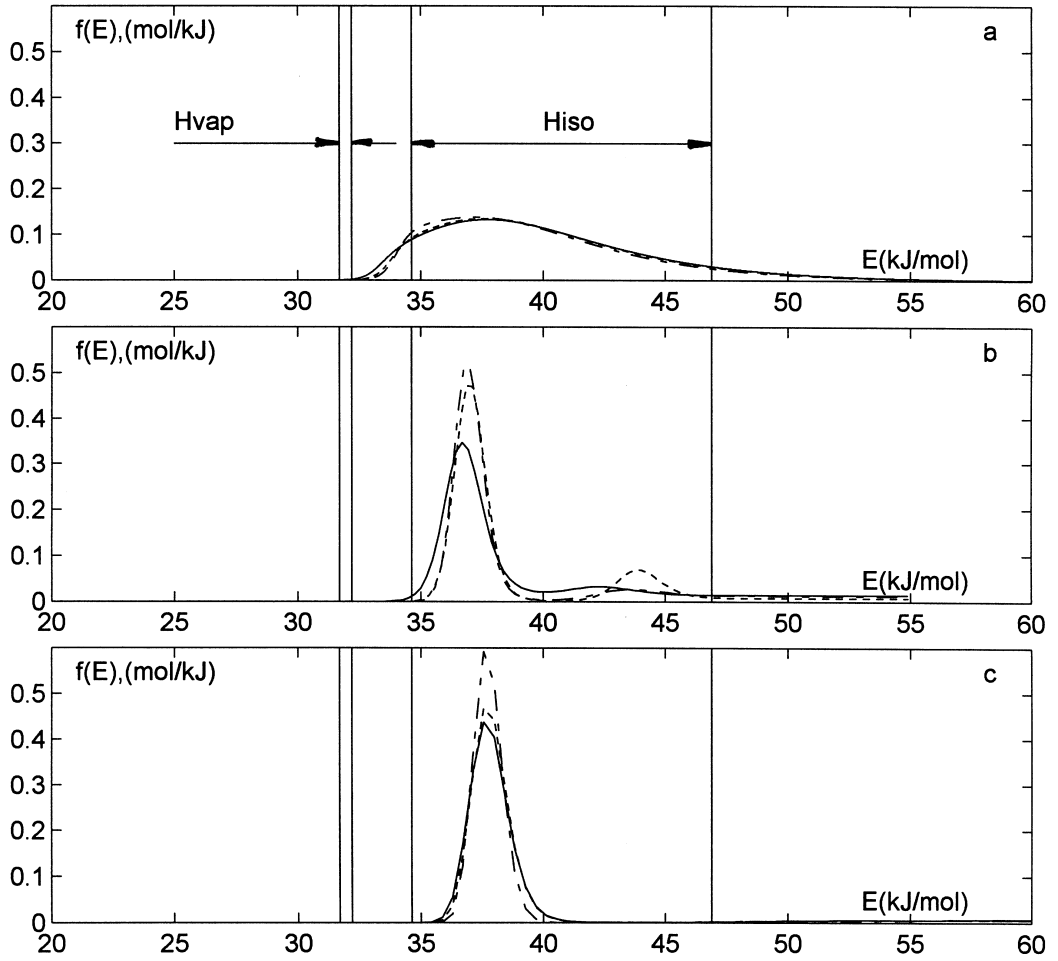

Fig. 3. Adsorption energy distributions of $CHCl_3$ at 288K (solid line), 293K (short-dashed line) and 298K (long-dashed line) calculated for the Jovanovic–Freundlich model (a), by the EM method with the Jovanovic isotherm as local model (b) and by the EM method with the Langmuir isotherm as local model (c).

corresponding amount adsorbed at the given pressure. These latter q_{cal} values were then used in Eq. (15) to produce the corresponding root-square-mean-deviation ($\delta_{JF,\lambda(\epsilon)}$). The values of $\delta_{JF,\lambda(\epsilon)}$ are exposed in column 5 of Table 1. This calculation permits to check if any information is lost during the inversion of Eq. (11). The numerical inversion was carried out using a precision which assured on one hand a reasonable match between the values of (δ_{JF}) and ($\delta_{JF,\lambda(\epsilon)}$) and on the other hand a good approximation of the normalization condition (8).

Also, the corresponding root-square-mean-deviation values are reported for the EM models for Langmuir (δ_L) and Jovanovic local behavior (δ_J) in columns 5 and 8 of Table 2, respectively. For the particular case of chloromethane, the calculated adsorption isotherms obtained within the framework of the EM method (using Eq. (12)) are shown for Jovanovic (Fig. 7a) and for Langmuir (Fig. 7b) local behavior, respectively, along with the experimental data points.

We can also define an experimental root-square-mean-deviation for each set (constant temperature) of data as

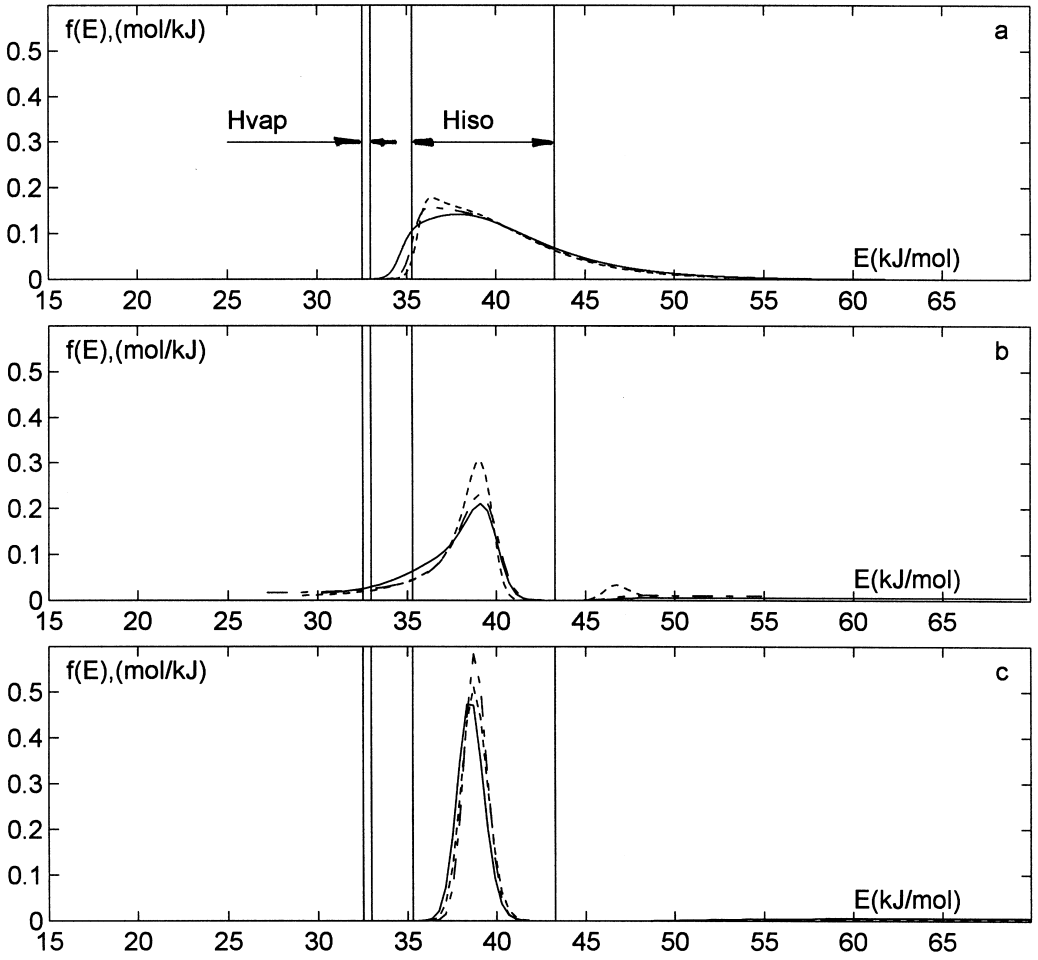

Fig. 4. Adsorption energy distributions of CCl_4 at 288K (solid line), 293K (short-dashed line) and 298K (long-dashed line) calculated for the Jovanovic–Freundlich model (a), by the EM method with the Jovanovic isotherm as local model (b) and by the EM method with the Langmuir isotherm as local model (c).

$$\delta_{exp} = \sqrt{\sum \left(\frac{\Delta q_{exp}}{q_{exp}} \right)^2} \quad (16)$$

where $\frac{\Delta q_{exp}}{q_{exp}}$ is the relative error of the experimental data. The data is reported to have an average error less than 1% over the entire adsorption range [9,10]. So a maximum value of $\frac{\Delta q_{exp}}{q_{exp}}$ can be set equal to 0.01. Then, a rough estimate of δ_{exp} can be done as

$$\delta_{exp} = 0.01\sqrt{N} \quad (17)$$

where N is the number of experimental points for the given isotherm. The values of δ_{exp} calculated for each experimental isotherm are reported in the last column of Table 1.

4. Discussion

Figs. 1a–6a show that the AEDs corresponding to the JF model with Jovanovic local behavior are single-peak quasi-Gaussian functions, more or less skewed in the direction of the high adsorption

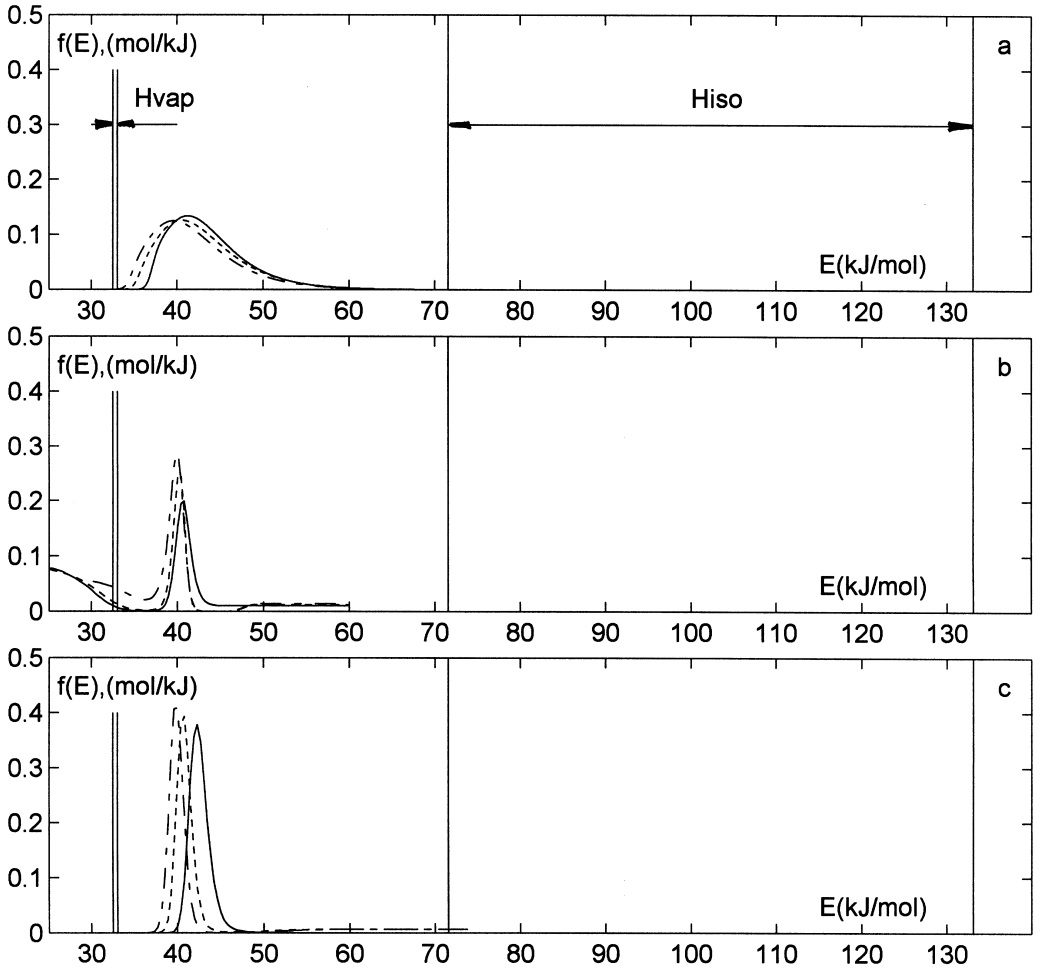

Fig. 5. Adsorption energy distributions of $C_2H_3Cl_3$ at 288K (solid line), 293K (short-dashed line) and 298K (long-dashed line) calculated for the Jovanovic–Freundlich model (a), by the EM method with the Jovanovic isotherm as local model (b) and by the EM method with the Langmuir isotherm as local model (c).

energies. In some cases, the distributions are only mildly unsymmetrical, showing the highest degree of asymmetry near the base of the peak. It is worth noting at this point that this behavior reminds the behavior of the AEDs corresponding to the Langmuir–Freundlich [4] model for Langmuir local behavior, which are quasi-Gaussian symmetrical functions [4]. The parallelism between the behavior of the two models is somehow related to the fact that the Jovanovic–Freundlich model reduces to the Jovanovic model when the surface becomes homogeneous while the Langmuir–Freundlich model reduces to the Langmuir model when the surface becomes homogeneous. Note also that both the Jovanovic–Freundlich and the Langmuir–Freundlich models reduce to the monolayer at high pressures but do not reduce to the Henry law at low coverages [4,7].

Figs. 1a–6a show that the adsorption energy distributions calculated for the analyzed species at three different temperatures are very similar in terms of shape and location on the energy axis. Similar results were obtained previously at different temperatures for the same set of experimental data with energy distribution functions represented either by a Morse-type [9] or exponential decay [7] functions. These facts indicate that for the Jovanovic–Freund-

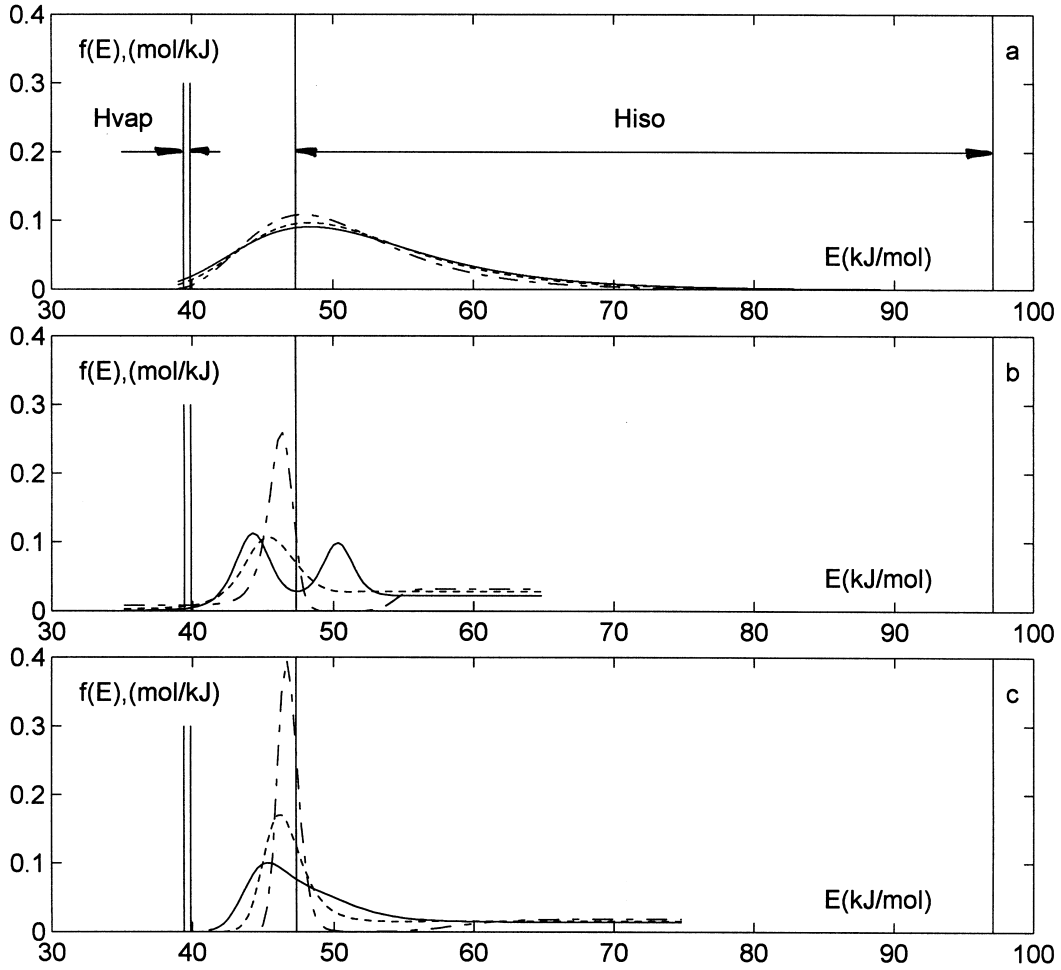

Fig. 6. Adsorption energy distributions of C_2Cl_4 at 288K (solid line), 293K (short-dashed line) and 298K (long-dashed line) calculated for the Jovanovic–Freundlich model (a), by the EM method with the Jovanovic isotherm as local model (b) and by the EM method with the Langmuir isotherm as local model (c).

lich model the energy distribution functions are almost temperature independent. In this sense, the model behaves in the same fashion as other models do, as suggested elsewhere [4]. This situation is possibly related to the fact that there are only small differences between the values of the heterogeneity parameter for the same compound at different temperatures (See Table 3 from Ref. [7]). Also, the temperature range in which the original data was obtained is relatively small (10°C) and it is reasonable to think that big differences should not be expected for the specific case under study. Moreover, the numerical values of the heterogeneity parameter are close for the different compounds. The highest value obtained was for chloromethane ($\nu \approx 0.8$), thus producing the narrowest energy distribution (Fig. 1a). The lowest value was for tetrachloroethylene ($\nu \approx 0.4$), which gives the broadest energy distribution (Fig. 6a). Note that dichloromethane and carbon tetrachloride ($\nu \approx 0.7$) and trichloromethane and 1,1,1-trichloroethane ($\nu \approx 0.6$) give energy distributions which exhibit a similar dispersion (see Figs. 2a–5a). These findings confirm that for the Jovanovic–Freundlich model the AEDs narrow with the increase in the value of the heterogeneity parameter. Also in this sense, the model behaves in the

Table 1
Results derived from the analysis of the experimental data for the JF model

Adsorbate	T (K)	$\epsilon_{a,\mathrm{JF}}$ (kJ/mol)	δ_{JF}	$\delta_{\mathrm{JF},f(e)}$	δ_{exp}
CH_3Cl	288	24.7	0.2601	0.2633	0.0374
CH_3Cl	293	24.7	0.4492	0.4530	0.0387
CH_3Cl	298	24.8	0.5802	0.5840	0.0436
CH_2Cl_2	288	32.9	0.1501	0.1532	0.0374
CH_2Cl_2	293	32.9	0.2297	0.2332	0.0387
CH_2Cl_2	298	32.6	0.3062	0.3103	0.0374
$CHCl_3$	288	36.3	0.1018	0.0978	0.0332
$CHCl_3$	293	36.3	0.1121	0.1080	0.0332
$CHCl_3$	298	36.2	0.1755	0.1822	0.0316
CCl_4	288	36.9	0.0978	0.1037	0.0332
CCl_4	293	37.1	0.1715	0.1807	0.0332
$C_2H_3Cl_3$	288	39.8	0.0504	0.0505	0.0374
$C_2H_3Cl_3$	293	38.9	0.1109	0.1109	0.0400
$C_2H_3Cl_3$	298	38.0	0.1093	0.1140	0.0412
C_2Cl_4	288	46.3	0.0313	0.1147	0.0374
C_2Cl_4	293	46.1	0.0315	0.0861	0.0374
C_2Cl_4	288	45.8	0.1472	0.1609	0.0412

same fashion as other reported well known models [4].

Another interesting finding is that the JF model predicts a similar degree of adsorbent heterogeneity for all the systems analyzed, all the AEDs derived having a similar shape, as reported previously [7,9]. There is, of course, a shift of the density functions along the energy axis produced as a consequence of the different values of the characteristic energy ϵ_a, which characterizes the position of the maximum of the energy distributions. This result is also similar to other ones previously reported [7,9]. From the results reported in Table 1 and Figs. 1–6 it is clear that the order of decreasing adsorption strength of the ana-

Table 2
Results derived from the analysis of the experimental data for the EM models

Adsorbate	T (K)	$q_{s,\mathrm{L}}$ (mmol/g)	$\epsilon_{\mathrm{mean,L}}$ (kJ/mol)	δ_{L}	$q_{s,\mathrm{J}}$ (mmol/g)	$\epsilon_{\mathrm{mean,J}}$ (kJ/mol)	δ_{J}
CH_3Cl	288	7.03	26.0	0.0101	6.54	25.1	0.0020
CH_3Cl	293	7.05	25.8	0.0171	6.14	25.2	0.0072
CH_3Cl	298	6.88	35.6	0.0329	5.82	25.3	0.0223
CH_2Cl_2	288	5.93	34.4	0.0184	4.99	34.0	0.0069
CH_2Cl_2	293	5.98	34.2	0.0244	4.89	33.9	0.0114
CH_2Cl_2	298	5.84	33.8	0.0333	4.81	33.6	0.0158
CH_2Cl_3	288	3.97	37.8	0.0159	3.55	36.9	0.0049
$CHCl_2$	293	3.93	37.9	0.0222	3.47	37.1	0.0075
$CHCl_3$	298	3.87	377.8	0.0244	3.41	37.0	0.0073
CCl_4	288	3.17	38.6	0.0168	2.97	37.6	0.0086
CCl_4	293	3.10	38.8	0.0330	2.84	37.9	0.0221
CCl_4	298	3.00	38.8	0.0214	2.81	37.8	0.0129
$C_2H_3Cl_3$	288	3.46	42.8	0.01118	3.54	41.1	0.0050
$C_2H_3Cl_3$	293	3.48	40.9	0.0256	3.57	40.2	0.0152
$CC_2H_3Cl_3$	298	3.51	39.9	0.0187	3.51	39.6	0.0092
C_2Cl_4	288	3.00	52.6	0.0085	2.87	44.2	0.0071
C_4Cl_4	293	2.94	477.2	0.0053	2.82	46.6	0.0025
C_2Cl_4	298	2.87	46.8	0.0247	2.72	45.8	0.0148

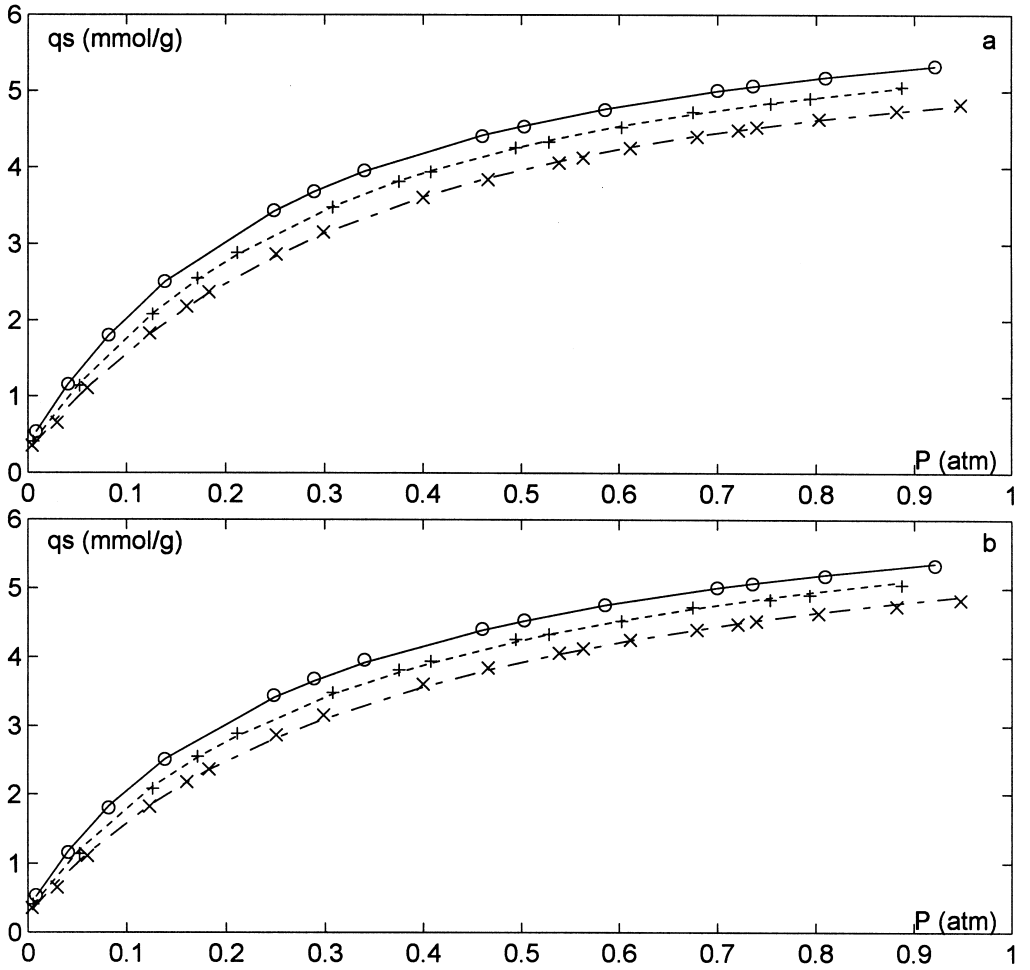

Fig. 7. Fit of the adsorption isotherm data of CH_3Cl at 288 K (solid line), 293 K (short-dashed line) and 298 K (long-dashed line) by the EM method with the Jovanovic isotherm as local model (a) and by the EM method with the Langmuir isotherm as local model (b). Experimental data points also represented by 288 K (○), 293 K (+) and 298 K (×).

lyzed species is given as follows: $C_2Cl_4 > C_2H_3Cl_3 > CCl_4 \simeq CHCl_3 > CH_2Cl_2 > CH_3Cl$. Note that the same order roughly holds for the values of the corresponding heats of vaporization [17], which define the lowest boundary on the energy axis for the AEDs. Accordingly, the AEDs derived using the JF model (Figs. 1a–5a) show that the calculated adsorption energies are as a rule equal to or higher than the heats of vaporization. In the case of C_2Cl_4, there is a small part of the AED at energies less than the heat of vaporization. The effect is more pronounced for T=293 K and T=288 K while at T=298 K the problem is barely existent. Note from Table 1 that at T=293 K and T=288 K there is not a good match between the values of δ_{JF} and $\delta_{JF,\lambda(\epsilon)}$ for C_2Cl_4. This fact indicates that the numerical inversion of the Laplace transform in Eq. (11) is not efficient in these cases. Note that there exist a reasonable agreement between the values of δ_{JF} and $\delta_{JF,\lambda(\epsilon)}$ for the rest of the systems exposed in Table 1. So, the numerical inversion of the Laplace transform is adequate for the majority of the systems. Note also that for C_2Cl_4 at T=293 K and T=288 K the values of δ_{JF} are less than δ_{exp}. So the model errors are less than the estimated experimental errors, thus the possibility of some ''modeling'' of the experimental errors is

Table 3
Check of the normalization condition for the different models

Adsorbate	T (K)	$\int \lambda_{JF}(\varepsilon)\, d\varepsilon$	$\int \lambda_{J}(\varepsilon)\, d\varepsilon$	$\int \lambda_{L}(\varepsilon)\, d\varepsilon$
CH_3Cl	288	0.9997	0.8100	0.9978
CH_3Cl	293	0.997	0.9047	0.9982
CH_3Cl	298	0.9998	0.9620	0.9985
CH_2Cl_2	288	0.9994	0.9987	0.9990
CH_2Cl_2	293	0.9994	0.9987	0.9983
CH_2Cl_2	298	0.9994	0.9988	0.9995
$CHGl_3$	288	1.0018	0.996	0.9977
$CHCl_3$	293	1.0018	0.9992	0.9984
$CHCl_3$	298	0.9981	0.9986	0.9992
CCl_4	288	0.9976	0.9629	1.0002
CCl_4	293	0.9983	0.9671	0.9984
CCl_4	298	0.9983	0.9281	1.0006
$C_2H_3Cl_3$	288	0.9978	0.6576	1.0011
$C_2H_3Cl_3$	293	0.9994	0.6428	0.9996
$C_2H_3Cl_3$	298	0.9967	0.9448	0.9975
C_2Cl_4	288	0.9593	0.9914	0.9981
C_2Cl_4	293	0.9758	0.9842	0.9959
C_2Cl_4	298	0.9892	0.9686	0.9978

possible for these cases. For the remaining systems $\delta_{JF} > \delta_{exp}$. From column 3 of Table 3 it is additionally evident that there is a satisfactory compliance with the normalization condition for all the systems with the exception of C_2Cl_4 at T = 293 K and T = 288 K. This situation results from the fact that the distributions are slightly truncated at the low energy end. So, the fact that the inversion produces some values of energies less than the heat of vaporization can be just an artifact. It is possible that the situation is somehow related to the ''overfiting'' of the experimental data by the model. Recall that the inversion of Eq. (11) is an ill posed problem difficult to circumvent in every situation.

The results obtained with the EM method using the Langmuir local behavior are reasonably consistent. They are illustrated in Figs. 1c–6c. There is often a small amount of adsorption at energies higher than those of the main peak. This high adsorption energy was not well characterized and could correspond to a second type of high energy sites. However, there was insufficient data at very low pressures to allow the derivation of numerical estimates in this region. The energy range was expanded in the direction of high energies in order to better visualize the main, low energy peak, which was present no matter the width of the range used. The adsorption at high energy, however, was not contained in the low-energy first peak and can be ''diluted'' as the energy scale is expanded to higher energies. This is indicative of insufficient experimental data to characterize the low pressure (high energy) region of adsorption. The energies of adsorption for the AEDs derived for Langmuir local behavior are always greater than the corresponding heats of vaporization. These AEDs are almost symmetrical for the majority of the systems (see Figs. 1c–6c) with the sole exception of C_2Cl_4 at 288 K. Note that the EM method with Langmuir local behavior produce errors δ_L as a rule less than the experimental errors δ_{exp}. The order of both types of errors seems to be the same. Moreover, because the values of δ_{exp} are just approximate, maximum estimates it is reasonable to think that there is a reasonable agreement between the model errors and experimental errors for the case of the EM method with Langmuir local behavior. The lowest model errors are again the values corresponding to C_2Cl_4 at T = 293 K and T = 288 K. The normalization condition holds very well for this model, as seen from column 5 of Table 3. The results obtained with the EM algorithm for the case of Jovanovic local behavior are different than those obtained for a Langmuir local model. They are illustrated in Figs. 1b–6b. A better fit was obtained with the Jovanovic than with the Langmuir isotherm as the local model,

as shown by the fact that $\delta_J < \delta_L$ for all the systems. Note also that $\delta_J < \delta_{exp}$ for all systems. The AEDs corresponding to the Jovanovic local behavior are not symmetrical for several systems and in some cases possess a multipeak character (see Figs. 2b, 3b, 4b, 6b). In some cases (Figs. 1b, 4b, 6b and especially 5b) the low energy region was not represented as well with the Jovanovic model as it was with the Langmuir model. As seen from the figures, the values of the AEDs do not approach to a low value when the value of the energy approaches the value of the heat of vaporization. Basically, the distributions are truncated at the ϵ_{min} endpoint. This fact is reflected in the value of the normalization integral (column 4 of Table 3). The obtained multipeak distributions and energies of adsorption less than the corresponding heats of vaporization are possibly not real physicochemical features of the studied systems but most likely artifacts arising from the fact that the Jovanovic local model forces its associated AED to sample such low values of energy that improve the fit of the experimental data. So, the EM method simply tries to fit the data as best as possible in accordance with the model chosen, and possibly overfits it, modeling also the experimental errors. These artifacts are very common. It is noteworthy to recall at this point that the parameters obtained from the fit of the given experimental data to the Hines model [9] also produced AEDs sampling energies of adsorption less than the heat of vaporization [9]. The majority of the AEDs derived from the EM method for both Langmuir and Jovanovic local behavior are similar for different temperatures. The major exception are the distributions calculated for C_2Cl_4 (Figs. 6b and 6c). Note from Table 2 that model errors are very small for these cases. The problem is more serious for the EM method for Jovanovic local behavior. The drawback in using a direct technique to obtain AEDs like the EM procedure is that any inconsistencies or systematic errors present in the data, even if they are small also get modeled. Artifacts are problematic when solving ill-posed problems and it is the price usually paid. Note that the Jovanovic–Freundlich model (Fig. 6a) produces AEDs very similar at different temperatures. Note that an overall analysis of the model errors shows that $\delta_{JF} > \delta_L > \delta_J$ and that the appearance of artifacts increases going from the JF model to the EM model with Jovanovic local behavior. So, the result of a ''too good'' fitting of the experimental data is possibly the appearance of artifacts. Despite the artifacts present in some AEDs, it is noteworthy that the AEDs calculated by the three different methods applied in this study occupy the very same range of the energy axis. Note the similarities among the values of $\epsilon_{mean,L}$; $\epsilon_{mean,J}$ and $\epsilon_{a,JF}$ shown in Tables 1 and 2. This is a consistent result. Moreover, for the majority of the systems, this range also contains the values determined experimentally for the isosteric heats of adsorption [9,10], as shown in Figs. 1–6. The agreement obtained is quite reasonable if one considers that the experimental isosteric heats of adsorption were determined using the intermediate region of the adsorption isotherm [9,10]. Thus, values of the isosteric heats below and above the reported range are possible. The only exception is the AED of $C_2H_3Cl_3$ for which the AEDs calculated by the three different methods used here do not contain the range of experimental values of the isosteric heat of adsorption (Fig. 5). It is difficult to supply at this time an unbiased explanation to this fact. However, it is worth noting that a previous identification procedure, applying a linearized version of Eq. 3, provided values of the characteristic energies lower or close to the energies of vaporization for all the compounds with the exception of $C_2H_3Cl_3$ (Table 8 from Ref. [7]). This Table shows also that the values of ϵ_a were determined with an important error, possibly because the three temperatures at which the isotherms were obtained were too close (288 K, 293 K and 298 K). Thus, the linear plots of ln a versus $1/RT$ were almost horizontal (see Fig. 2 from ref. [7]). The value of ϵ_a for $C_2H_3Cl_3$ is the highest (ca. 80 kJ/mol) and was determined with the smallest error (see Table 8 from Ref. [7]). If we use this latter value of the characteristic energy in Eq. (11) in order to approximate the value of $\frac{a}{K_0}$ as $e^{\frac{\epsilon_a}{RT}}$, we obtain the AEDs displayed in Fig. 8a, which contains the range in which the isosteric heats of adsorption were reported. The AEDs calculated by the three methods applied in this study are of course different, as should be expected given the different nature of the three models compared. All of them are just approximations of the actual AEDs. Yet, all the distributions

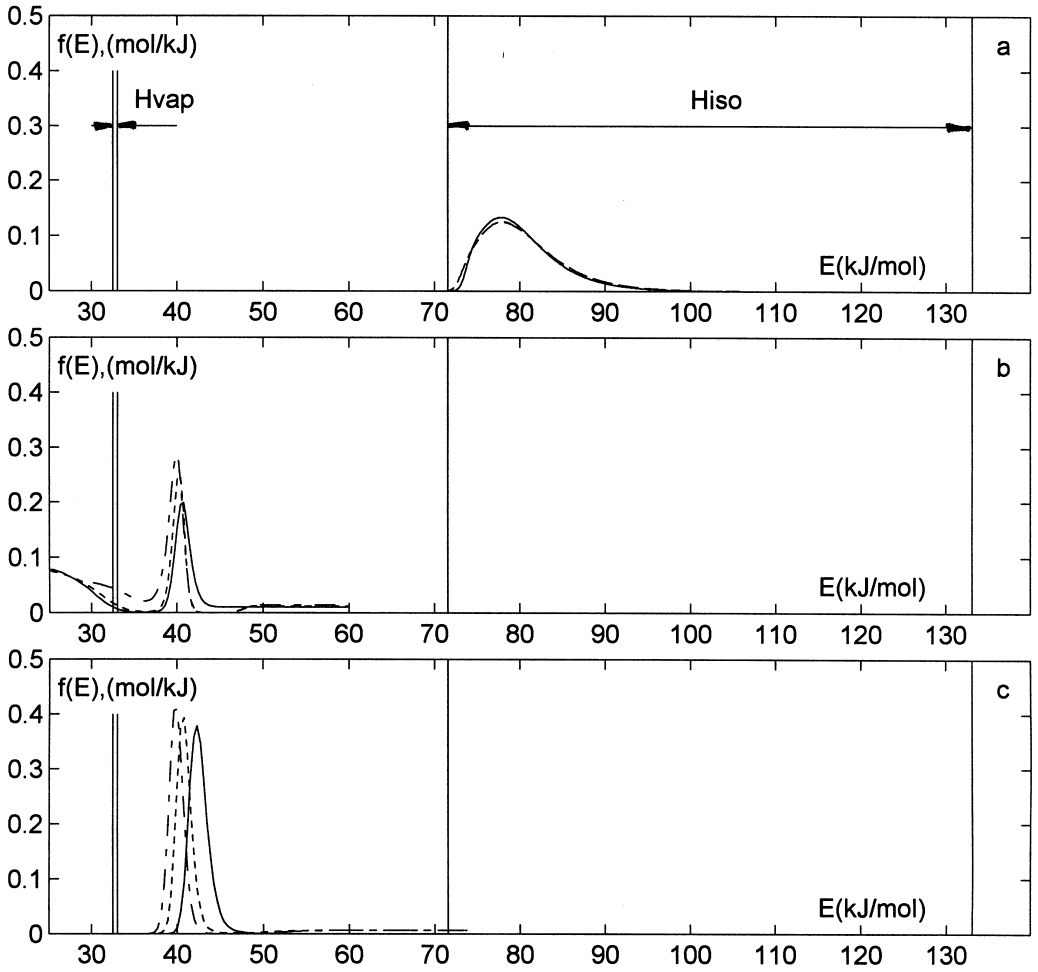

Fig. 8. Adsorption energy distributions of $C_2H_3Cl_3$ at 288 K (solid line), 293 K (short-dashed line) and 298 K (long-dashed line) calculated for the Jovanovic–Freundlich model (a), by the EM method with the Jovanovic isotherm as local model (b) and by the EM method with the Langmuir isotherm as local model (c).

occupy the same range of values on the energy axis, which coincides with the range where the isosteric heats of adsorption were experimentally determined. The fact that the JF model, which is simpler, gives results similar to the ones derived from more complex models (the EM approach) encourages the possible use of this model in the correlation of single component data and as a tool to extract information regarding adsorbent heterogeneity, that could be useful in the prediction of multicomponent equilibria. As a matter of fact, the multicomponent extension of the Jovanovic–Freundlich model (2) was reported recently [20] both for systems without and with lateral interactions on the surface. The models were applied with satisfactory results to competitive adsorption data of phenyl alcohols on a C-18 reversed-phase from methanol/water solutions [20]. The aforementioned study also compared the performance of the JF model with other global isotherms for heterogeneous surfaces. The parameters present in the competitive global isotherm were directly related to the single component Jovanovic–Freundlich model which accounts for the heterogeneity of the surface. These multicomponent

equilibrium models can be used in the calculation of overloaded chromatographic band profiles [2]. Finally, it is interesting to correlate the heterogeneity parameter, ν, and some experimental parameter characterizing the adsorption systems studied (see Table 4). The dipole moments (μ) and the Van der Waals volumes (V_{vdw}) of the solutes [17] cannot be expected to correlate well with the surface heterogeneity, especially in the case of a series of light chlorinated hydrocarbons. For these compounds, the Van der Waals volume depends essentially on the number of chlorine atoms (Table 4) while the isosteric heat of adsorption (ΔH_{iso}) depends on the number of atoms which can interact with the surface at a given time. The dipole moment depends on the geometrical structure of the molecule and its symmetry. It is very different for $CHCl_3$ and CCl_4 while the adsorption energies are close, as expected (Table 4). The ratio $\Delta H_{iso}/\Delta q_{iso}$ of the difference between the minimum and the maximum value of the isosteric heat of adsorption to the corresponding difference between the amounts adsorbed (i.e., q_{iso}) or change of the isosteric heat of adsorption per unit increase of loading gives an approximate idea of the dispersion of the energy distribution in the range investigated. Table 4 compares this ratio and the average values of the heterogeneity parameter, $\bar{\nu}$, identified from the fit of the Jovanovic–Freundlich model [7], at the different temperatures studied. The last two columns of the Table correlate nicely. As explained earlier, the dispersion of the AED increases with decreasing value of ν while the ratio $\Delta H_{iso}/\Delta q_{iso}$ is zero for a homogeneous surface and increases with increasing heterogeneity. Together with the excellent agreement between the range of energies occupied by the calculated AEDs and the range of isosteric heats of adsorption experimentally determined by Hines et al. [9,10] (Figs. 1–6), this correlation suggests that our results are consistent with the experimental data and reasonable.

5. Conclusions

The adsorption energy distributions corresponding to the Jovanovic–Freundlich model with Jovanovic local behavior were determined from the adsorption data of a series of chlorinated hydrocarbons on silica gel. These AEDs were derived from the best isotherms using a numerical inversion of the Laplace transform. The AED are single-peak functions skewed in the direction of high energies. They are nearly temperature independent and the values calculated for the adsorption energies are higher than the heats of vaporization of the corresponding compound at the same temperature. It was established that the dispersion of the distribution decreases with increasing value of the heterogeneity parameter of the Jovanovic–Freundlich model. All this results are consistent with the behavior of other models reported for single component adsorption on heterogenous surfaces [4]. On the other hand, the results presented here and in a previous study [7] show that the calculation of the AEDs is biased by the selection of the local isotherm model. This fact complicates the assessment of the true energy distribution.

It is worth noting that the AEDs corresponding to the JF model occupies a range of adsorption energies which is the same as the one occupied by the AEDs calculated from the raw adsorption data using other reported procedures like the EM method, which makes no assumption regarding the nature of the

Table 4
Some properties of the adsorbate and the adsorption system

Adsorbate	μ (D)	V_{VdW} (m^3/kmol)	H_{iso} (kJ/mol)	q_{iso} (mmol/g)	$\Delta H_{iso}/\Delta q_{iso}$ (kJ·g/mol^2)	ν
CH_3Cl	1.87	0.02529	26.63–27.13	2.0–4.5	200.00	0.77
CH_2Cl_2	1.60	0.03471	38.77–43.17	2.0–4.5	1760.00	0.69
$CHCl_3$	1.01	0.04350	34.63–46.89	1.4–3.3	6452.63	0.62
CCl_4	0.00	0.0523	35.30–43.29	0.9–2.4	5326.67	0.69
$C_2H_3Cl_3$	1.78	0.05372	71.60–133.15	1.2–2.4	51291.67	0.58
C_2Cl_4	0.00	0.05898	47.31–97.14	1.6–2.4	62287.50	0.42

overall isotherm. Additionally, this range also overlaps with the range of probable values derived from the experimental results for the isosteric heats of adsorption. Thus, the JF model being a rather simple analytical model gives a meaningful interpretation of the energy distribution. It also could be a useful choice for the correlation of single component data and subsequent prediction of multicomponent adsorption data within the framework of existing models which incorporate the effect of surface heterogeneity [5,6,20]. These multicomponent equilibrium adsorption data can then be used in connection with appropriate models of chromatography to calculate overloaded multicomponent band profiles in preparative and industrial chromatography [2]. Although the results of this study are directly applicable for gas or vapor phase separations only, it is possible that a careful extrapolation of the formalism can be accomplished for liquid phase separations.

Acknowledgements

This work has been supported in part by Grant CHE-97-01680 of the National Science Foundation and by the cooperative agreement between the University of Tennessee and the Oak Ridge National Laboratory. We acknowledge the support of Maureen S. Smith in solving our computational problems.

References

[1] S.C. Stinson, Chem. Eng. News 73 (1995) 44.
[2] G. Guiochon, S.G. Shirazi, A.M. Katti, Fundamentals of Nonlinear and Preparative Chromatography, Academic Press, Boston, 1994.
[3] D.P. Valenzuela, A.L. Myers, Adsorption Equilibrium Data Handbook, Prentice Hall, Englewood Cliffs, 1989.
[4] M. Jaroniec, R. Madey, Physical Adsorption On Heterogeneous Solids, Elsevier, Amsterdam, 1998.
[5] D.P. Valenzuela, A.L. Myers, O. Talu, I. Zwiebel, AIChE J. 34 (1988) 397.
[6] F. Karavias, A.L. Myers, Chem. Eng. Sci. 47 (1992) 1441.
[7] I. Quiñones, G. Guiochon, J. Colloid and Interf. Sci. 183 (1996) 57.
[8] R. Sips, J. Chem. Phys. 16 (1948) 490.
[9] S.–L. Kuo, A.L. Hines, N.H. Dural, Separat. Sci. Technol. 26 (1991) 1077.
[10] S.–L. Kuo, A.L. Hines, J. Chem. Eng. Data 37 (1992) 1.
[11] B. Stanley, G. Guiochon, Langmuir 10 (1994) 4279.
[12] B. Stanley, G. Guiochon, J. Phys. Chem. 97 (1993) 8098.
[13] D.S. Jovanovic, Kolloid–Z. Z. Polym. 235 (1969) 1203.
[14] M. Jaroniec, Surf. Sci. 50 (1975) 553.
[15] S. Sircar, A.L. Myers, Surf. Sci. 205 (1988) 353.
[16] E.C. Titchmarsh, Introduction To the Theory of Fourier Integrals, Oxford Univ. Press, London, 1959.
[17] T.E. Daubert, R.P. Danner, Physical and Thermodynamic Properties of Pure Chemicals, Hemisphere Publishing Company, New York, 1989.
[18] Anon., IMSL Inc., ''FORTRAN subroutines for mathematical applications V2.0: User's Manual'', MATH/LIBRARY, Houston, 1991.
[19] I. Langmuir, J. Am. Chem. Soc. 40 (1918) 1361.
[20] I. Quiñones, G. Guiochon, J. Chromatogr. A 796 (1998) 15.